



HAL
open science

On the multistream approach of relativistic Weibel instability. I. Linear analysis and specific illustrations

Alain Ghizzo, Pierre Bertrand

► **To cite this version:**

Alain Ghizzo, Pierre Bertrand. On the multistream approach of relativistic Weibel instability. I. Linear analysis and specific illustrations. *Physics of Plasmas*, 2013, 20 (8), pp.082109. 10.1063/1.4817750 . hal-01769689

HAL Id: hal-01769689

<https://hal.science/hal-01769689>

Submitted on 18 Apr 2018

HAL is a multi-disciplinary open access archive for the deposit and dissemination of scientific research documents, whether they are published or not. The documents may come from teaching and research institutions in France or abroad, or from public or private research centers.

L'archive ouverte pluridisciplinaire **HAL**, est destinée au dépôt et à la diffusion de documents scientifiques de niveau recherche, publiés ou non, émanant des établissements d'enseignement et de recherche français ou étrangers, des laboratoires publics ou privés.

On the multistream approach of relativistic Weibel instability. I. Linear analysis and specific illustrations

A. Ghizzo, and P. Bertrand

Citation: [Physics of Plasmas](#) **20**, 082109 (2013); doi: 10.1063/1.4817750

View online: <https://doi.org/10.1063/1.4817750>

View Table of Contents: <http://aip.scitation.org/toc/php/20/8>

Published by the [American Institute of Physics](#)

Articles you may be interested in

[On the multistream approach of relativistic Weibel instability. III. Comparison with full-kinetic Vlasov simulations](#)
Physics of Plasmas **20**, 082111 (2013); 10.1063/1.4817752

[On the multistream approach of relativistic Weibel instability. II. Bernstein-Greene-Kruskal-type waves in magnetic trapping](#)
Physics of Plasmas **20**, 082110 (2013); 10.1063/1.4817751

[Multidimensional electron beam-plasma instabilities in the relativistic regime](#)
Physics of Plasmas **17**, 120501 (2010); 10.1063/1.3514586

[Three-dimensional Weibel instability in astrophysical scenarios](#)
Physics of Plasmas **10**, 1979 (2003); 10.1063/1.1556605

[On the role of the purely transverse Weibel instability in fast ignitor scenarios](#)
Physics of Plasmas **9**, 2458 (2002); 10.1063/1.1476004

[Collisionless Weibel shocks: Full formation mechanism and timing](#)
Physics of Plasmas **21**, 072301 (2014); 10.1063/1.4886121



**COMPLETELY
REDESIGNED!**

**PHYSICS
TODAY**

Physics Today Buyer's Guide
Search with a purpose.

On the multistream approach of relativistic Weibel instability.

I. Linear analysis and specific illustrations

A. Ghizzo and P. Bertrand

Institut Jean Lamour-UMR 7168, University of Lorraine, BP 239 F-54506 Vandoeuvre les Nancy, France

(Received 16 May 2013; accepted 15 July 2013; published online 9 August 2013)

A one-dimensional multistream formalism is extended for the study of temperature anisotropy driven Weibel-type instabilities in collisionless and relativistic plasma. The formulation is based on a Hamiltonian reduction technique using the invariance of generalized canonical momentum in transverse direction. The Vlasov-Maxwell model is expressed in terms of an ensemble of one-dimensional Vlasov-type equations, coupled together with the Maxwell equations in a self-consistent way. Although the model is fundamentally nonlinear, this first of three companion papers focuses on the linear aspect. Dispersion relations of the Weibel instability are derived in the linear regime for different kinds of polarization of the electromagnetic potential vector. The model allows new unexpected insights on the instability: enhanced growth rates for the Weibel instability are predicted when a dissymmetric distribution is considered in \mathbf{p}_\perp . In the case of a circular polarization, a simplification of the linear analysis can be obtained by the introduction of the “multiring” approach allowing to extend the analytical model of Yoon and Davidson [Phys. Rev. A **35**, 2718 (1987)]. Applications of this model are left to the other two papers of the series where specific problems are addressed pertaining to the nonlinear and relativistic dynamics of magnetically trapped particles met in the saturation regime of the Weibel instability. © 2013 AIP Publishing LLC.

[<http://dx.doi.org/10.1063/1.4817750>]

I. INTRODUCTION

The classic Weibel instability is a purely growing electromagnetic mode excited in an unmagnetized plasma by perpendicular free energy, stored in the velocity anisotropy of plasma particles. The free energy source for the instability is provided by a temperature anisotropy of the electron distribution function between the perpendicular and longitudinal directions in the momentum space. A substantial fraction of the kinetic energy of the plasma is thus converted into the generation of strong quasi-static magnetic fields through the redistribution of currents in space. This instability was first predicted by Weibel in Ref. 1 for a non relativistic plasma. A simple physical interpretation provided the same year by Fried in Ref. 2 treated the particle distribution anisotropy more generally as a two-stream configuration of a cold plasma. This second kind of instability is usually referred as the current filamentation instability (CFI). In CFI the instability is then driven by velocity (or momentum) anisotropy instead of the standard temperature anisotropy.

The physical mechanisms underlying the development of both CFI and WI are very similar and are found in the redistribution of particle currents inside the system. Such an aspect underlies the similarities between WI and CFI instabilities and allowed us to build a theoretical model based on a multistream description allowing to unify both types of instabilities. We underline that, as a consequence of the strong physical and mathematical analogies, CFI is often called Weibel instability, in particular in the laser-plasma interaction context. Here, CFI appears as a consequence of the acceleration of a “hot” electron bunch that induces a colder, although denser return current in order to maintain quasi-neutrality. Moreover, this sort of situation occurs in the fast ignition

scenario, where the charge of the relativistic electron beam is compensated by the return current. On the other hand, in the astrophysical context, WI and CFI are involved in the birth of cosmological magnetic field. Theoretically, such Weibel-type instabilities are capable to create the seed magnetic field in the large interpenetrating structures of intergalactic plasmas. Some investigations have proposed the relevance of WI for the generation of magnetic fields in gamma-ray bursters in Refs. 3–6 or galaxy cluster shocks.⁷

While Weibel-type instabilities have been introduced fifty years ago, there are many questions to be answered. For instance, it is worth noting that the relativistic formulation of the Weibel instability remains a complex problem since the temperature anisotropy cannot be easily introduced starting from the standard Maxwell-Jüttner distribution. When relativistic effects must be taken into account, the problem is additionally complicated by the nonlinear dependence of the energy of particles on their momentum and the strong coupling between perpendicular and parallel momenta through the relativistic Lorentz factor. The first discussion of the relativistic formulation of the Weibel instability is by Yoon and Davidson in Ref. 8 where the stability of a “ring” in momentum was studied. This model combines a Water-Bag^{9,10} description in the longitudinal direction and a cold Dirac-type distribution in the perpendicular direction. Indeed, this model can be considered as a simplified version of the multistream model, first introduced in Ref. 11 and applied for the study of CFI in Ref. 12 and for WI in the non relativistic regime in Ref. 13.

Furthermore, the standard Weibel instability is usually non resonant with plasma particles: assuming a complex frequency ω , WI grows exponentially in time with a growth

rate given by $Im(\omega) > 0$, while the real part $Re(\omega) = 0$. However, the features of WI can be modified and a resonant regime occurs when the instability is coupled with a parallel two-stream instability as shown by Lazar *et al.* in Ref. 14. Thus for large wave numbers, the aperiodic feature of WI changes and the instability becomes oscillatory in time exhibiting now a finite real frequency $Re(\omega) \neq 0$. This so-called resonant regime is typically encountered in a counter-streaming plasma when the stream velocities are fast enough. On the other hand when the two stream instability is introduced in the perpendicular direction of \mathbf{k} (and now referred as CFI), i.e., when both filamentation and Weibel instabilities are emitted in the same direction, a cumulative effect was observed in Ref. 15, leading to an enhanced growth rate larger than those observed for pure filamentation and pure Weibel instabilities. However, in the former situation, the CFI mode exhibits a hybrid electrostatic—electromagnetic nature leading to the excitation of the plasma wave. Such a coupling with the plasma wave is also met in the asymmetric distributions which require the need of new analytical tools making the calculations more tractable in relativistic situations.

Our model is thus based on a full kinetic description of the dynamics in the longitudinal direction (here denoted p_x), while a Hamiltonian reduction is used to select a class of exact solutions to describe the dynamics in the perpendicular direction in terms of a sum of particle “bunches” or “streams.” The material is presented in three companion papers. Our model can be used to determine first in paper I the linear dispersion relation in a more tractable way allowing to take into account dissymmetric distributions. The second paper II in Ref. 16 address the physics that ultimately limits the growth of WI and deals with the stability of non-linear Bernstein-Greene-Kruskal (BGK)¹⁷ in a magnetic version at saturation of Weibel-type instabilities. The third paper, part III in Ref. 18 is based on numerical comparisons between a numerical version of the multistream model with full kinetic Vlasov-Maxwell simulations in the relativistic regime of WI. The paper is organised as follows. We briefly present our Hamiltonian model in Sec. II. The linear analysis is presented in Sec. III. To simplify the analysis, we have chosen to keep the water-bag description for the longitudinal direction (although there is no restriction in the kinetic treatment in p_x) and to put the emphasis on the multistream approach in the perpendicular directions, showing that both methods, “water bag” and “stream” differ in a fundamental way. In Sec. IV, we come back to the concept of temperature and finally discuss the relevance of this approach to specific relativistic distributions showing the correspondence in the sense of the moments. Section V is devoted to the study of a symmetric distribution function in momentum, while the case of a dissymmetric distribution is considered in Sec. VI. In Sec. VII, the multistream model is extended to the concept of “rings” in the perpendicular momentum (p_y, p_z) space allowing to take into account circularly polarized waves showing that the multistream model can be seen as a generalisation of Yoon’s and Davidson’s model presented in Ref. 8. Conclusions are given in Sec. VIII. Some auxiliary calculations are also presented in appendixes.

II. THE MULTISTREAM MODEL

Here, we sum up the basic equations used in the multistream model. We restrict our analysis to plane waves propagating along the x -direction assuming ions as a fixed neutralising background. Let us consider the Hamiltonian of one particle, of rest mass m and charge e , in the electromagnetic field (\mathbf{E}, \mathbf{B})

$$H = mc^2(\gamma - 1) + e\phi(x, t), \quad (1)$$

where the standard value of the Lorentz factor is given by

$$\gamma = \left[1 + \frac{p^2}{m^2 c^2} \right]^{1/2}. \quad (2)$$

In Refs. 11–13, we have shown that, it is possible to reduce the dimension of the global phase space by using the invariance of the canonical momentum

$$\mathbf{P}_{c\perp} = \mathbf{p} + e\mathbf{A}_\perp = \text{const} = \mathbf{C}_j, \quad (3)$$

in the perpendicular direction. Such a property results from the fact that the Hamilton’s equation is zero ($d\mathbf{P}_{c\perp}/dt = -\partial H/\partial \mathbf{q}_\perp = 0$) since the Hamiltonian is assumed to depend only on the longitudinal spatial coordinate, here denoted x . Thus without loss of generality, we can consider a plasma where the particles are divided into $2N + 1$ “bunches” or “streams” of particles, each “stream” j (for $|j| \leq N$) having the same initial perpendicular momentum \mathbf{C}_j . We can now define, for a particle population j , a distribution function noted $f_j(x, p_x, t)$ which satisfies the following relativistic Vlasov-type equation:

$$\frac{\partial f_j}{\partial t} + \frac{p_x}{m\gamma_j} \frac{\partial f_j}{\partial x} + \left(eE_x - \frac{1}{2m\gamma_j} \frac{\partial}{\partial x} (\mathbf{C}_j - e\mathbf{A}_\perp)^2 \right) \frac{\partial f_j}{\partial p_x} = 0, \quad (4)$$

where the Lorentz factor γ , initially given by Eq. (2), becomes now

$$\gamma_j = \left[1 + \frac{p_x^2}{m^2 c^2} + \frac{(\mathbf{C}_j - e\mathbf{A}_\perp(x, t))^2}{m^2 c^2} \right]^{1/2}. \quad (5)$$

Thus for each population j , the source terms used in the Maxwell equations are defined as

$$n_j(x, t) = \int_{-\infty}^{+\infty} f_j(x, p_x, t) dp_x, \quad (6)$$

$$\mathbf{J}_{\perp j} = \frac{e}{m} (\mathbf{C}_j - e\mathbf{A}_\perp) \int_{-\infty}^{+\infty} \frac{f_j}{\gamma_j} dp_x, \quad (7)$$

respectively for the density and the perpendicular current density. Finally, the reduced Vlasov equations given by Eq. (4) are self-consistently coupled to the Poisson equation and the potential vector \mathbf{A}_\perp

$$\frac{\partial E_x}{\partial x} = \frac{e}{\epsilon_0} \left(\sum_{j=-N}^{+N} n_j(x, t) - n_0 \right), \quad (8)$$

$$\frac{\partial^2 \mathbf{A}_\perp}{\partial t^2} - c^2 \frac{\partial^2 \mathbf{A}_\perp}{\partial x^2} = \frac{1}{\epsilon_0} \sum_{j=-N}^N \mathbf{J}_{\perp j}(x, t), \quad (9)$$

allowing to reduce the phase space to 2D one x, p_x , plus $2N + 1$ values for the corresponding \mathbf{C}_j vector.

Notice that this model has been applied intensively for the study of wave-particle resonances in laser-plasma interaction using only a single stream, i.e., a cold Dirac-type distribution function in the perpendicular momentum direction. While restricted to a spatially periodic conditions in Ref. 19, the code has been successfully extended to a non periodic causal bounded system in Ref. 20, allowing the code to deal with more realistic and longer plasma. The case of the extension to the relativistic regime of laser-plasma interaction is studied in Ref. 21.

III. LINEAR ANALYSIS AND “MULTIFLUID” APPROACH

Although our model takes into account a continuous distribution in p_x , we choose to follow Yoon and Davidson and to introduce here a Water-Bag description in the longitudinal direction (here denoted p_x), while keeping the concept of the multistream for \mathbf{p}_\perp . While the (multiple) water-bag model is based on the Liouville’s theorem (see Ref. 22 for more details) and the resulting conservation of the particle distribution function, the multistream model uses the invariance of the perpendicular canonical momentum vector and the model keeps its kinetic character even with one stream. The evolution of the particle population can be described by the distribution of type

$$F(x, p_x, p_y, t) = \sum_{j=-N}^{+N} F_j [\mathcal{H}(p_x + p_j^+) - \mathcal{H}(p_x - p_j^-)] \delta(\mathbf{p}_\perp - (\mathbf{C}_j - e\mathbf{A}_\perp)), \quad (10)$$

where \mathcal{H} is the Heaviside function. We assume that $p_j^\pm = \pm p_{aj}$ initially at time $t=0$. In the water-bag approach, it is sufficient to follow the dynamics of the contours, here obtained by determining the different moments of the reduced Vlasov equations (4). We obtain thus

$$\frac{\partial p_j^\pm}{\partial t} + \frac{p_j^\pm}{m\gamma_j^\pm} \frac{\partial p_j^\pm}{\partial x} = eE_x - \frac{1}{2m\gamma_j^\pm} \frac{\partial}{\partial x} (\mathbf{C}_j - e\mathbf{A}_\perp(x, t))^2, \quad (11)$$

where the longitudinal electric field E_x and the transverse potential vector \mathbf{A}_\perp are, respectively, given by Eqs. (8) and (9). Here, γ_j^\pm is the Lorentz factor, corresponding to the stream j and the water-bag contours p_j^\pm , given by

$$\gamma_j^\pm = \left[1 + \frac{p_j^{\pm 2}}{m^2 c^2} + \frac{(\mathbf{C}_j - e\mathbf{A}_\perp(x, t))^2}{m^2 c^2} \right]^{1/2}. \quad (12)$$

A physically equivalent approach would consist in considering a multifluid model described by the set of Eqs. (11) coupled with the field equations (8) and (9). Note that this system is closed. For the analytical study, this hydrodynamical formulation of the multistream model is particularly convenient. In the case of a linear normal mode analysis, we assume for the stream j that $p_j^\pm = \pm p_{aj} + \delta p_j^\pm$, $n_j = n_{0j} + \delta n_j$, $\mathbf{A}_\perp = \delta \mathbf{A}_\perp$, $E_x = \delta E_x$ and by using the definition of

the distribution F given in Eq. (10), the set of Eqs. (8), (9), and (11) becomes now

$$\frac{\partial \delta p_j^\pm}{\partial t} \pm \frac{p_{aj}}{m\Gamma_{aj}} \frac{\partial \delta p_j^\pm}{\partial x} = e\delta E_x + \frac{e}{m\Gamma_{aj}} \mathbf{C}_j \cdot \frac{\partial}{\partial x} \delta \mathbf{A}_\perp, \quad (13)$$

$$\frac{\partial \delta E_x}{\partial x} = \frac{e}{\epsilon_0} \sum_{j=-N}^{+N} F_j (\delta p_j^+ - \delta p_j^-), \quad (14)$$

$$\frac{\partial^2 \delta \mathbf{A}_\perp}{\partial t^2} - c^2 \frac{\partial^2 \delta \mathbf{A}_\perp}{\partial x^2} = \frac{e}{m\epsilon_0} \sum_{j=-N}^N (\mathbf{C}_j - e\delta \mathbf{A}_\perp) \rho_j, \quad (15)$$

with the relative density ρ_j of stream j given by

$$\rho_j = \int_{-\infty}^{+\infty} \frac{f_j}{\gamma_j} dp_x = mcF_j \int_{u_j^-}^{u_j^+} \frac{du_x}{\sqrt{1 + u_x^2 + \mathbf{a}_{j\perp}^2}}. \quad (16)$$

Here, we have used the simplified (normalized) notation: $u_j^\pm = p_j^\pm/mc$, $\mathbf{a}_{j\perp} = (\mathbf{C}_j - e\mathbf{A}_\perp)/mc$ and $u_x = p_x/mc$. After calculating the integral in Eq. (16), we obtain for the relative density the following expression:

$$\rho_j = mcF_j \ln \left(\frac{u_j^+ + \gamma_j^+}{u_j^- + \gamma_j^-} \right). \quad (17)$$

In Eq. (13), the Lorentz factor Γ_{aj} is given by

$$\Gamma_{aj} = \sqrt{1 + \frac{p_{aj}^2}{m^2 c^2} + \frac{\mathbf{C}_j^2}{m^2 c^2}}. \quad (18)$$

The expression of the Lorentz factor in Eq. (12) allows us to rewrite the analytical form of ρ_j in a more tractable form. By denoting $\gamma_j^\pm = \Gamma_{aj} + \delta\gamma_j^\pm$ in a perturbative form, a little algebra leads to the following expression for the relative density:

$$\rho_j = n_{0j} \alpha_j \langle \gamma_{aj}^{-1} \rangle + \frac{n_{0j} \alpha_j}{2u_{aj}} \frac{\delta p_j^+ - \delta p_j^-}{mc\Gamma_{aj}} + \frac{en_{0j} \alpha_j \mathbf{C}_j \cdot \delta \mathbf{A}_\perp}{m^2 c^2 \Gamma_{aj} \left(1 + \frac{\mathbf{C}_j^2}{m^2 c^2} \right)}, \quad (19)$$

where we have used

$$\delta\gamma_j^\pm = \pm \frac{p_{aj} \delta p_j^\pm}{m^2 c^2 \Gamma_{aj}} - \frac{e\mathbf{C}_j \cdot \delta \mathbf{A}_\perp}{m^2 c^2 \Gamma_{aj}}. \quad (20)$$

In Eq. (19), the term $\langle \gamma_{aj}^{-1} \rangle$ is defined in the standard way

$$\langle \gamma_{aj}^{-1} \rangle = \frac{1}{2u_{aj}} \ln \left(\frac{1 + \beta_{aj}}{1 - \beta_{aj}} \right) = \frac{1}{\Gamma_{aj}} G(\beta_{aj}), \quad (21)$$

using the notation of a normalized velocity $\beta_{aj} = v_{aj}/c = u_{aj}/\Gamma_{aj}$. The function G , of argument β , is defined as follows:

$$G(\beta) = \frac{1}{2\beta} \ln \left(\frac{1 + \beta}{1 - \beta} \right). \quad (22)$$

By linearizing the previous set of equations given by Eqs. (13)–(15), using the standard notation $\delta = \exp i(kx - \omega t)$, we get the following system:

$$\left(1 - \omega_p^2 \sum_{j=-N}^N \frac{\alpha_j}{\Gamma_{aj}(\omega^2 - k^2 v_{aj}^2)}\right) \delta E_x - ik\omega_p^2 \sum_{j=-N}^N \frac{\alpha_j}{m\Gamma_{aj}^2} \frac{C_j \delta A_\perp}{\omega^2 - k^2 v_{aj}^2} = 0 \quad (23)$$

$$\begin{aligned} & -ik\omega_p \sum_{j=-N}^N \frac{\alpha_j C_j}{m\Gamma_{aj}^2(\omega^2 - k^2 v_{aj}^2)} \delta E_x \\ & - \omega_p^2 k^2 \sum_{j=-N}^N \frac{\alpha_j C_j (C_j \delta A_\perp)}{m^2 \Gamma_{aj}^3(\omega^2 - k^2 v_{aj}^2)} + (\omega_k^2 - \omega^2) \delta A_\perp \\ & - \frac{e}{m\epsilon_0} \sum_{j=-N}^N \alpha_j \langle \gamma_{aj}^{-1} \rangle C_j + \omega_p^2 \sum_{j=-N}^N \frac{\alpha_j C_j (C_j \delta A_\perp)}{m^2 c^2 \Gamma_{aj} \left(1 + \frac{C_j^2}{m^2 c^2}\right)} = 0. \end{aligned} \quad (24)$$

Here, the quantity $\alpha_j = 2p_{aj}F_j/n_0$ represents the normalized density of the stream j (such quantities verify indeed the normalization condition $\sum_{j=-N}^{+N} \alpha_j = 1$). We have also introduced the frequency of the electromagnetic wave ω_k , which is given in the usual form

$$\omega_k^2 = \omega_p^2 \sum_{j=-N}^{+N} \alpha_j \langle \gamma_{aj}^{-1} \rangle + k^2 c^2. \quad (25)$$

Now, by considering that the determinant of the system formed by Eqs. (23) and (24) is zero, it is possible to obtain a simple expression of the dispersion relation for WI in the relativistic regime. However, we adopt to simplify here the presentation just by choosing the simplified version of a linearly polarized wave, i.e., by assuming that the potential vector perturbation writes now $\delta A_\perp = \delta A_y e_y$. The case of a circularly polarized wave will be studied later in Sec. VII. Here, we assume that the net current is zero or equivalently

$$\sum_{j=-N}^N \alpha_j C_j \langle \gamma_{aj}^{-1} \rangle = 0. \quad (26)$$

A little algebra leads to the general expression of the dispersion relation in a more compact formulation

$$\begin{aligned} & \left[\omega^2 - \omega_k^2 + \omega_p^2(\omega^2 - k^2 c^2) \sum_{j=-N}^{+N} \frac{\alpha_j C_j^2}{m^2 c^2 \Gamma_{aj} \left(1 + \frac{C_j^2}{m^2 c^2}\right)} (\omega^2 - k^2 v_{aj}^2) \right] \\ & \times \left[1 - \omega_p^2 \sum_{j=-N}^N \frac{\alpha_j}{\Gamma_{aj}(\omega^2 - k^2 v_{aj}^2)} \right] \\ & = k^2 \omega_p^4 \left[\sum_{j=-N}^N \frac{\alpha_j C_j}{m\Gamma_{aj}^2(\omega^2 - k^2 v_{aj}^2)} \right]^2. \end{aligned} \quad (27)$$

When the stream repartition in the p_y -space is symmetric (the right-hand term of Eq. (27) is therefore zero), both electrostatic (ES) and electromagnetic (EM) modes are then uncoupled. While the electrostatic mode (with $\delta E_x \neq 0$ and $\delta A_y = 0$) obeys the dispersion relation

$$1 - \omega_p^2 \sum_{j=-N}^{+N} \frac{\alpha_j}{\Gamma_{aj}(\omega^2 - k^2 v_{aj}^2)} = 0, \quad (28)$$

the electromagnetic mode including the Weibel instability is given by

$$\begin{aligned} & \omega^2 - \omega_k^2 + \omega_p^2(\omega^2 - k^2 c^2) \\ & \times \sum_{j=-N}^{+N} \frac{\alpha_j C_j^2}{m^2 c^2 \Gamma_{aj} \left(1 + \frac{C_j^2}{m^2 c^2}\right)} (\omega^2 - k^2 v_{aj}^2) = 0. \end{aligned} \quad (29)$$

Notice that in the cold limit where $p_{aj} \rightarrow 0$, the dispersion relation given by Eq. (27) looks like the dispersion relation of CFI in Ref. 23.

IV. MOMENTS OF THE DISTRIBUTION FUNCTION IN THE MULTISTREAM MODEL

In the kinetic version of the multistream model presented in Sec. II, we can keep a full Vlasov description in the longitudinal direction (here denoted p_x), the temperature is then described in a standard way using the data of the different distribution functions $f_j(x, p_x, t)$, which depend explicitly of the p_x variable. Now, in the perpendicular p_y direction, the concept of temperature may be recovered by considering the moments of the distribution function, or in other words, by looking at the equivalence in the fluid moment sense of the multistream distribution and a continuous version of the distribution function. To this purpose, let us consider the case of a cold distribution function in p_x but keeping a relativistic temperature in p_y . In this section of the paper, we choose to normalize the frequency ω , the wave vector k , momentum $p_{x/y}$ and C_j respectively to the plasma frequency ω_p , the electron skin depth c/ω_p and to mc . We have also introduced the normalized velocity $\beta = v/c$. The equilibrium distribution corresponds to:

$$F_0(p_x, p_y) = \frac{n_0}{2K_1(\mu)} e^{-\mu\sqrt{1+p_y^2}} \delta(p_x), \quad (30)$$

with the standard definition of $\mu = mc^2/T_y$. Thus by defining the quantity $h(p_y) = \int F_0(p_x, p_y) dp_x$, we can use for the multistream model the following functional form:

$$h(p_y) = \sum_{j=-N}^N F_j \delta(p_y - C_j). \quad (31)$$

We then defined the $2n$ -moment of the quantity $h(p_y)$ as

$$\left\langle \frac{p_y^{2n}}{\gamma} \right\rangle = \int_{-\infty}^{+\infty} \frac{p_y^{2n} h(p_y) dp_y}{\gamma} = \sum_{j=-N}^N \frac{C_j^{2n} F_j}{\sqrt{1+C_j^2}} = \sum_{j=-N}^N \frac{C_j^{2n} F_j}{\Gamma_j}, \quad (32)$$

where we have defined the Lorentz factor Γ_j by $\Gamma_j = \sqrt{1 + C_j^2}$. By introducing the notation $\alpha_j = F_j/n_0$, the equivalence condition for the two first non zero moments $\langle p_y^2/\gamma \rangle$ and $\langle p_y^4/\gamma \rangle$ of the distribution F_0 leads to

$$\left\langle \frac{p_y^2}{\gamma} \right\rangle = \frac{1}{\mu} = \sum_{j=-N}^N \frac{C_j^2 \alpha_j}{\Gamma_j}, \quad (33)$$

$$\left\langle \frac{p_y^4}{\gamma} \right\rangle = \frac{3K_2(\mu)}{2\mu^2 K_1(\mu)} = \sum_{j=-N}^N \frac{C_j^4 \alpha_j}{\Gamma_j}, \quad (34)$$

together with the normalization condition

$$\sum_{j=-N}^N \alpha_j = 1. \quad (35)$$

Here $K_n(\mu)$ is the modified Bessel function of second kind of order n . Now, we assume that the j -stream verifies the following symmetry properties $C_{-j} = -C_j$ and $\alpha_{-j} = \alpha_j$ for every values of j between 1 to N . We take also $C_0 = 0$ for the central beam. Now by restricting the system to a three-stream model, Eqs. (33) and (34) become now

$$\frac{2C_1^2 \alpha_1}{\Gamma_1} = \frac{1}{\mu}, \quad (36)$$

$$\frac{2C_1^4 \alpha_1}{\Gamma_1} = \frac{3K_2(\mu)}{2\mu^2 K_1(\mu)}. \quad (37)$$

The quantities C_1 and α_1 , together with α_0 define the different streams in the three-stream model. Dividing Eq. (37) by Eq. (36), we have $C_1 = -C_{-1} = \sqrt{3K_2(\mu)/2\mu K_1(\mu)}$ and $\alpha_1 = \alpha_{-1} = \Gamma_1/(\mu C_1^2)$. For the central stream we recall that $C_0 = 0$ and that α_0 can be calculated from Eq. (35). Thus, we have here $\alpha_0 = 1 - 2\Gamma_1/(\mu C_1^2)$. While in the Maxwell-Jüttner distribution in Eq. (30), the quantity μ^{-1} defines the effective kinetic temperature in the perpendicular direction as:

$$\frac{T_y}{mc^2} = \frac{1}{n_0} \iint \frac{p_y^2}{\sqrt{1 + p_y^2}} F_0(p_x, p_y) dp_x dp_y = \frac{1}{\mu}, \quad (38)$$

in the non-continuous version, the concept of temperature can be recovered by the ‘‘spacing’’ of streams in the perpendicular momentum space. For the three-stream model, it is the spacing of the streams $j = \pm 1$ which plays this role; the central beam having finally no contribution. In the multistream model, the perpendicular temperature can be defined as

$$\frac{T_y}{mc^2} = \sum_{j=-N}^N \frac{C_j^2 \alpha_j}{\Gamma_j} = \frac{1}{\mu}. \quad (39)$$

In the general case with $2N + 1$ streams, the system of Eqs. (33)–(35) may be generalized and takes the form of a Vandermonde system. In particular, when trying to solve this system numerically, it becomes ill-conditioned for large

values of the number of streams. A more convenient way can be found for the resolution of the system for a large number of streams and for a regular sampling of the p_y axis, i.e., for an equispaced set of C_j values. The idea is then to compute the F_j values at points $C_j = j\Delta C$ (using for instance $\Delta C \sim \frac{1}{2}p_{th,y}$ where $p_{th,y}$ is the thermal momentum along the y axis) for a given distribution function. We will see that such an approximation becomes accurate for a total number of streams greater than five, at least in the linear regime. These results will be used in paper III to initiate the plasma using a more general shape of equilibrium distribution introduced by Schlickeiser in Ref. 24 taken into account a temperature anisotropy in generalized Maxwell-Jüttner-type distribution. As mentioned previously, the part III companion paper¹⁸ presents numerical comparison with full kinetic Vlasov-Maxwell simulations.

V. THE SYMMETRIC CASE: PURE TRANSVERSE WI

Let us consider the linear dispersion relation for the relativistic regime given in Eq. (29) in presence of stream symmetry in the p_y direction which indeed is a particular case of the coupled ES/EM dispersion relation (27). Notice that the second member of Eq. (27) becomes zero when the repartition of the C_j values is symmetrical in p_y . The analytical formulation of the linear dispersion (27) as a discrete summation over an assembly of streams provides a general and exact approach to take into account any type of anisotropy of the distribution function. The case of CFI, involving two cold beams, was recently treated in Ref. 12.

As a first application of WI, let us consider the case where $\beta_{aj} = 0$. In that case, Eq. (29) can be rewritten in a dimensionless polynomial form of fourth degree. One thereby gets the following dispersion relation:

$$\omega^4 - \omega^2 \left(\omega_k^2 - \sum_{j=-N}^{+N} \frac{\alpha_j C_j^2}{\Gamma_j (1 + C_j^2)} \right) - k^2 \sum_{j=-N}^{+N} \frac{\alpha_j C_j^2}{\Gamma_j (1 + C_j^2)} = 0, \quad (40)$$

where the frequency, wave vector, and velocity are normalized to ω_p , $d_e = c/\omega_p$ and c . Equation (40) has two real roots ω_1^2 and ω_2^2 such that

$$\omega_1^2 \omega_2^2 = -k^2 \sum_{j=-N}^{+N} \frac{\alpha_j C_j^2}{\Gamma_j (1 + C_j^2)} < 0, \quad (41)$$

showing that the system is always unstable. Such a polynomial equation in the case where $\beta_{aj} = 0$ presents the advantage of being solved for any value of the number of streams without difficulty since the order of the polynom does not depend of N . Thus, we can check the convergence of the model for a large number of streams. Finally, the numerical resolution of the dispersion relation given by Eq. (40) is performed under two initial techniques to build the position of streams corresponding to a Maxwell-Jüttner distribution of transverse temperature of $T_y = 2000$ keV. A graphical representation is given in Fig. 1 to aid comparison of the obtained convergence of the numerical solution when the number of

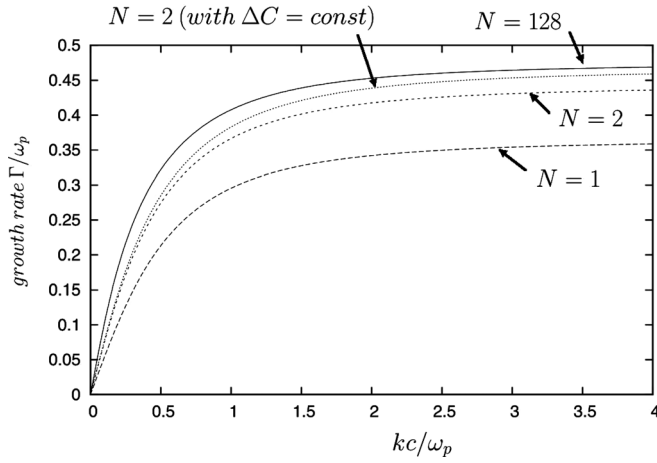


FIG. 1. Normalized growth rate $\frac{\Gamma}{\omega_p}$ versus $\frac{kc}{\omega_p}$. The solid line corresponds to the asymptotic solution reached for 15 streams using a regular sampling. The curve is identical using $N=128$ (i.e., 257 streams). The case of five streams is plotted in dotted line, unlike the dashed lines (below) are determined using the equivalence in the sense of the moments of f . It is necessary to use at least five streams when the equivalence in the sense of moments is used.

streams is modified. Fig. 1 displays the normalized growth rate Γ/ω_p as a function of the normalized wave number kc/ω_p . By choosing a regular sampling of the p_y axis (i.e., an equispaced set of C_j values, separated by $\Delta C \sim 0.50p_{th,y}$), the convergence is already obtained for $2N+1=15$ streams. We have represented in solid line the case of $2N+1=257$ streams (we have however used a smaller value of $\Delta C \sim 0.3$ which is identical to the case of 15 streams). The case of a regular sampling using five streams with $\Delta C = 0.75p_{th,y}$ ($p_{th,y} \simeq 4.032mc$) is plotted in dotted line. Note that the curve is very close of the exact solution plotted in solid line, even with a small number of streams.

Now let us consider the equivalence in the sense of the moments of the distribution. We have plotted the numerical solutions obtained using three streams (i.e., with $N=1$) and five streams (with $N=2$) in dashed lines, but now using the equivalence in the sense of the moments of f . In that case the initial position of streams C_j was determined by solving Eqs. (33)–(35) for three streams, or the system formed by Eqs. (32) and (35) when the number of stream is bigger than three. We observe that the convergence now is slow and the result obtained for three streams exhibits a non negligible error while the case $N=2$ (i.e., 5 streams) leads to a solution close to the expected value.

Hence, the case where $\beta_{aj} \neq 0$ corresponds now to a weaker anisotropy temperature, because we choose to keep the same perpendicular temperature but increases now the degree of the polynom form when the number of streams increases. We have tried three then five streams in Eq. (29). Thus, using a three-stream model in the transverse direction and a simplified water-bag description (with only one bag), we are able to recover the case of WI, driven by a temperature anisotropy if one of the roots is negative. We have shown, for a three-stream model that

$$\omega_1^2 \omega_2^2 = \omega_k^2 k^2 \beta_{a1}^2 - \frac{2\alpha_1 C_1^2 k^2}{\Gamma_{a1}(1+C_1^2)} < 0, \quad (42)$$

and we are able to recover the case of WI, driven by a temperature anisotropy if one of the roots is negative. From the last inequality (42), one gets the threshold condition of the temperature anisotropy necessary to initiate the instability in the relativistic regime.

The dispersion relation for seven streams is presented in Appendix A. The imaginary part of the stationary solution (the real part being zero) of the dispersion relation given by Eq. (A3) of the Appendix, for different sets of temperature parameters are plotted in Figs. 2 and 3 for the case of seven streams. Here, the equivalence in the sense of the moments has been used. Similar results have been obtained using five streams. Fig. 2 shows a typical plot of the growth rate Γ/ω_p against kc/ω_p for four different values of the longitudinal bag momentum p_a . Here the parameter p_a is kept fixed for each stream and p_a is taken from 0 till 1.5 by step of 0.5. When p_a increases, Fig. 2 confirms that the maximum growth rate of the instability shifts toward shorter wave numbers. In the above examples of Figs. 1 and 2, the perpendicular temperature of the distribution function is fixed to $T_y = 2000$ keV. Let us now remove such a constraint and consider the third example where T_y is now varying, while the longitudinal p_a value (and therefore the longitudinal temperature) is fixed to $p_a = 1.5$. The plot of the growth rate Γ/ω_p versus kc/ω_p , shown in Fig. 3, looks qualitatively similar to Fig. 2 and shows that the growth rate Γ decreases strongly when the perpendicular temperature decreases.

VI. THE DISSYMMETRIC CASE: CUMULATIVE EFFECT OF THE CFI AND WI GROWTH RATES

For completeness, now a relativistic distribution function is investigated that is asymmetric in momentum. The chosen distribution will couple linearly the filamentation and Weibel instabilities leading to a cumulative effect of these two instabilities. The cumulative effect is given by the solutions of Eq. (27), when the electrostatic branch is taken into account. Thus, the physical mechanism of WI and CFI are very similar and the amplification of the longitudinal plasma field has to be found in the symmetry breaking of the streams

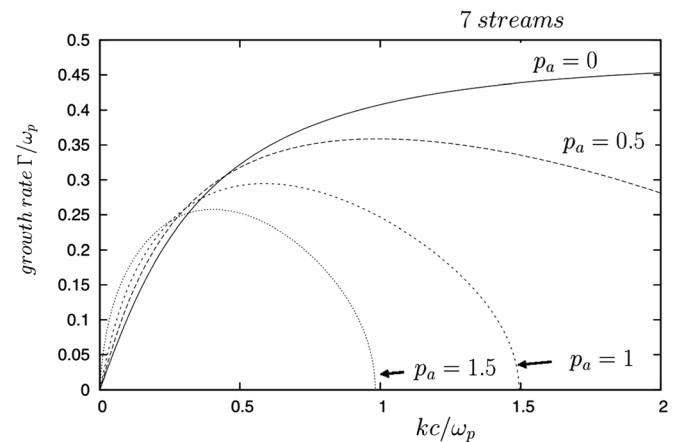


FIG. 2. Typical plot of the growth rate $\frac{\Gamma}{\omega_p}$ against $\frac{kc}{\omega_p}$ for four different values of the longitudinal bag momentum p_a , taken identical for the ensemble of streams. The perpendicular direction is described by seven streams, determined using the equivalence of the moments of the distribution function using Eq. (A3) in Appendix A. The perpendicular temperature is $T_y = 2000$ keV.

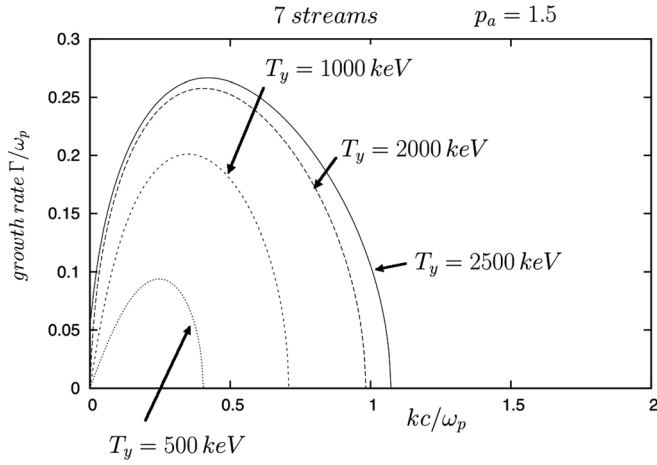


FIG. 3. Growth rate $\frac{\Gamma}{\omega_p}$ against $\frac{kc}{\omega_p}$ using seven streams from the resolution of the dispersion relation (A3) given in Appendix A for different values of the perpendicular temperature T_y . A water bag model with $p_a = 1.5mc$ is used in the longitudinal direction in p_x .

in the perpendicular momentum space. Note that a similar result was recently proposed by Bret *et al.* in Ref. 25 in the case of a shifted Maxwell-Jüttner distribution and previously by Tzoufras *et al.* in Ref. 26, this symmetry breaking being driven in the last situation, by space-charge effects. Furthermore, using a fluid cold relativistic model, Pegoraro

*et al.*²³ have already indicated such a behaviour of CFI in a situation somewhat different.

Let us now consider the coupling of both CFI and WI instabilities. Because we want to simplify the presentation, we do not take into account a longitudinal temperature and just consider the cold approximation (for p_x) of our multi-stream model. Thus, the Weibel instability is described in the standard way using $2N-1$ streams in the p_y direction, while CFI is exactly described by only the set of two streams. In other words, the dissymmetry in WI is here described by the introduction of only two non symmetric streams in the distribution of streams along the p_y direction. Of course, it is possible to take into account a more complex shape of the distribution function in p_y , by introducing a dissymmetry over many streams.

The resulting global distribution function, in the perpendicular direction p_y , is then described by the set of $2N+1$ “particle bunches” or streams, assuming that the right-hand side of the global dispersion relation, Eq. (27) is now different from zero through the presence of the term $(\sum_j \alpha_j C_j / \Gamma_j^2)^2 \neq 0$. Here $\Gamma_j = \sqrt{1 + C_j^2}$ is the normalized Lorentz factor obtained from Eq. (18) taking $p_{aj} = 0$. Equation (27) can be rewritten in a polynomial form of sixth degree. In a dimensionless expression, we get

$$\omega^6 + \omega^4 \left(-\omega_k^2 + \sum_{j=-N}^{+N} A_j - \sum_{j=-N}^{+N} \frac{\alpha_j}{\Gamma_j} \right) + \omega^2 \left(-k^2 \sum_{j=-N}^{+N} A_j + \omega_k^2 \sum_{j=-N}^{+N} \frac{\alpha_j}{\Gamma_j} - \sum_{j=-N}^{+N} \frac{\alpha_j}{\Gamma_j} \sum_{j'=-N}^{+N} \frac{\alpha_{j'}}{\Gamma_{j'}} \right) + k^2 \sum_{j=-N}^{+N} A_j \sum_{j'=-N}^{+N} \frac{\alpha_{j'}}{\Gamma_{j'}} - k^2 \left(\sum_{j=-N}^{+N} \frac{\alpha_j C_j}{\Gamma_j^2} \right)^2 = 0. \quad (43)$$

Here, we have assumed a charge neutrality condition and an initial zero net current $\sum_{j=-N}^{+N} \alpha_j C_j / \Gamma_j = 0$ while keeping $\sum_{j=-N}^{+N} \alpha_j C_j / \Gamma_j^2 \neq 0$. Here, the quantity A_j is given by Eq. (A4) in Appendix A, replacing Γ_{aj} by Γ_j .

We study the coupling of WI driven by a temperature anisotropy with $T_x = 0$ and $T_y = 2000$ keV coupled with CFI induced by two cold Dirac-type streams of respective momentum $p_1 = -0.8925$ and $p_2 = 20.40$ in mc -units. The corresponding beam densities are then $n_{01} = 0.60$ and $n_{02} = 0.40$ (with $n_{01} + n_{02} = 1$). These physical parameters have been determined assuming that the initial net current is zero for CFI, i.e., $n_{01} p_1 / \Gamma_1 = n_{02} p_2 / \Gamma_2$ and using the standard notation of the Lorentz factor Γ_j for each stream.

Concerning WI, we use $2N-1$ streams (here 127 streams) for describing the distribution function using equispaced C_j^{WI} invariants of the perpendicular canonical momentum. Thus, the values of the set of parameters $\{\alpha_j^{WI}, C_j^{WI}\}$, which describe WI for $|j| \leq N-1$, are obtained through the data of a Maxwell-Jüttner distribution and we have considered the case of a symmetric distribution given by $\alpha_{-j}^{WI} = \alpha_j^{WI}$ and $C_{-j}^{WI} = -C_j^{WI}$. We have chosen here $p_{aj}^{WI} = 0$ for the longitudinal direction. Thus we have built an initial distribution for both types of contribution, i.e., WI plus

CFI, having $2N+1$ streams globally and characterised by the set of parameters $\{\alpha_j, C_j\}$ chosen such that

$$C_j = C_j^{WI} \quad \text{for } |j| \leq N-1 \text{ for WI;} \\ C_{-N} = p_1 \text{ and } C_N = p_2 \quad \text{for CFI.} \quad (44)$$

The amplitude of streams is then defined by

$$\alpha_j = \alpha_j^{WI} (1 - \xi) \quad \text{for } |j| \leq N-1 \text{ for WI;} \\ \alpha_{-N} = n_{01} \xi \text{ and } \alpha_N = n_{02} \xi \quad \text{for CFI.} \quad (45)$$

The set of parameters $\{\alpha_j, C_j\}$ for $|j| \leq N$ verifies the two following conditions:

$$\sum_{j=-N}^{+N} \alpha_j = 1 \quad \text{and} \quad \sum_{j=-N}^{+N} \frac{\alpha_j C_j}{\Gamma_j} = 0. \quad (46)$$

Here the parameter ξ is the coupling coefficient for which WI is dominant for $\xi = 0$, while CFI is dominant for $\xi = 1$.

Fig. 4 displays the results. We point out that the growth rates of the mixed WI/CFI instability have their maximum for $kc/\omega_p \rightarrow +\infty$ as the result of the choice of the

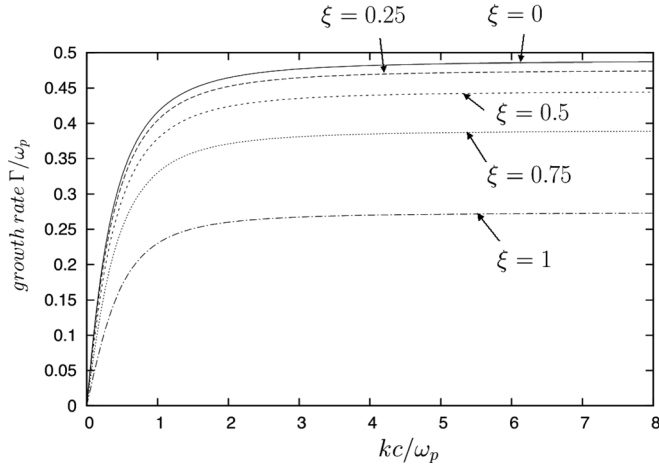


FIG. 4. Growth rate $\frac{\Gamma}{\omega_p}$ against $\frac{kc}{\omega_p}$ in the case of a mixed CFI-WI instability exhibiting an unexpected resonant character. The case $\xi = 0$ corresponds to a dominant WI while CFI is dominant for $\xi = 1$.

Dirac-type distribution in the p_x direction. In addition, we show that, for large wave numbers, the features of the WI instability changes and the mixed WI/CFI instability exhibits a cumulative effect in the sense that the growth rate is found larger than those of pure CFI and pure WI. For instance for $\xi = 0.50$ (i.e., $\sum_{j=-N+1}^{N-1} \alpha_j = \frac{1}{2}$ and $\alpha_N + \alpha_{-N} = \frac{1}{2}$, for the total contribution in amplitude for WI and CFI, respectively), the growth rate of the mixed instability is found close to $\Gamma_{WI+CFI}/\omega_p \simeq 0.44$, i.e., well above the linear expected value of $\frac{1}{2}(\Gamma_{WI} + \Gamma_{CFI})/\omega_p \simeq \frac{1}{2}(0.48 + 0.27) \simeq 0.375$, i.e., of the sum of both contributions taken alone without the coupling.

We have shown that the cumulative effect of the thermal anisotropy in presence of a dissymmetric streams leads to growing rates, which are markedly larger than those obtained in the same conditions for pure filamentation and Weibel instabilities. Here, the cumulative effect is linked to the growth of the Langmuir mode allowing to couple between both filamentation and Weibel instabilities. Notice that the excitation of a Langmuir wave may lead to a resonant-type instability in the sense that we expect wave-particle resonances in the non linear regime of the Weibel instability when the saturation is reached.

VII. CONCEPT OF “RING” FOR CIRCULARLY POLARIZED WAVE

It is instructive to consider, as an example, the case of a circularly polarized electromagnetic field. In the general case, the dispersion relation may be found from Eqs. (23) and (24) in the standard form of a matrix determinant equal to zero. The different coefficients of the tensor $\epsilon_{\alpha\beta}$ can be found in section B of appendix in Eqs. (B1)–(B4). Here, we assume again that we have the condition

$$\sum_{j=-N}^{+N} \alpha_j \mathbf{C}_j \langle \gamma_{aj}^{-1} \rangle = 0. \quad (47)$$

We see that, at least in the linear regime, the coupling with the longitudinal electric field is induced by the tensor

coefficient $\epsilon_{x\beta} = \epsilon_{\beta x}$ given by Eq. (B2) and we are faced with the same problem of the previous section where the coupling with the electrostatic mode is created by the non diagonal terms of the tensor $\epsilon_{\alpha\beta}$. If we assume now that both electromagnetic and electrostatic contributions are decoupled (WI becoming purely transverse), it is then possible to build the different streams repartitioned on several “rings” of radius $C_{\perp r}$. Thus for a class of streams $\{\alpha_j, \mathbf{C}_j\}$ having the same radius $C_{\perp r}$ ($C_{\perp r}$ being the modulus of the vector \mathbf{C}_j), we can introduce a random phase θ_j which determines the angular position of each stream on a given “ring” of label r . By conserving the central stream located at $C_0 = 0$, we can sample each ring by $2N/N_{ring}$ “streams” having the same $C_{\perp r}$ and where N_{ring} denotes the total number of considered rings. The canonical invariant writes then in the standard form in the perpendicular momentum space:

$$\mathbf{C}_j = C_{\perp r} \cos \theta_j \mathbf{e}_y + C_{\perp r} \sin \theta_j \mathbf{e}_z. \quad (48)$$

By averaging over the phase variable θ_j , it is then possible to recover the standard formalism of a purely transverse electromagnetic Weibel instability without amplification of an electrostatic component. By introducing an equilibrium distribution function in the form of a representation of N_{ring} circular rings:

$$F_0(p_x, p_{\perp}^2) = \sum_{r=0}^{N_{ring}} F_r [\mathcal{H}(p_x + p_{ar}) - \mathcal{H}(p_x - p_{ar})] \frac{\delta(p_{\perp} - C_{\perp r})}{2\pi p_{\perp}}, \quad (49)$$

it is possible to write the dispersion relation in the form

$$1 - \frac{k^2 c^2}{\omega^2} - \frac{\omega_p^2}{\omega^2} \sum_{r=0}^{N_{ring}} \frac{\alpha_r G(\beta_{ar})}{\Gamma_{ar}} - \frac{\omega_p^2}{\omega^2} (k^2 c^2 - \omega^2) \times \sum_{r=0}^{N_{ring}} \frac{\alpha_r \beta_{\perp r}^2}{2\Gamma_{ar} (1 - \beta_{ar}^2) (\omega^2 - k^2 c^2 \beta_{ar}^2)} = 0, \quad (50)$$

using the notation of Yoon and Davidson, i.e., $\langle \gamma_{ar}^{-1} \rangle = \frac{G(\beta_{ar})}{\Gamma_{ar}}$ and $\beta_{\perp r} = \frac{C_{\perp r}}{mc\Gamma_{ar}}$. Here, we use $\alpha_r = 2F_r p_{ar}/n_0$ and we have introduced the quantity $\beta_{ar} = p_{ar}/mc\Gamma_{ar}$ where the Lorentz factor Γ_{ar} is given by Eq. (18) by replacing the label j by r , which now determines the considered ring and by replacing the quantity $\mathbf{C}_j \cdot \mathbf{C}_j$ by $C_{\perp r}^2$. Note that the case $r=0$ corresponds to the central Dirac-type stream, located at the origin of the perpendicular momentum space with $C_{\perp 0} = 0$. The normalization condition of the distribution function leads to choose $\sum_{r=0}^{N_{ring}} \alpha_r = 1$. In the case where we consider only one ring and no central stream (i.e., assuming that $\alpha_0 = 0$ and $\alpha_1 = 1$), we recover the exact solution of Yoon and Davidson in Ref. 8. Indeed in the multistream model, we have assumed that each ring can be sampled by N_s streams using a Dirac-type distribution of parameters $\{\alpha_j, \mathbf{C}_j\}$ with $j = 1, \dots, N_s$ and $N_s = 2N/N_{ring}$ which obey the conditions $\sum_{j=1}^{N_s} \alpha_j = \alpha_r$ and \mathbf{C}_j is given by (48).

In the relativistic regime, the effective temperature in the perpendicular and parallel directions with respect to the wave vector direction is now defined by

$$\frac{T_{\perp}}{mc^2} = \int_0^{+\infty} dp_{\perp} 2\pi p_{\perp} \int_{-\infty}^{+\infty} dp_x \frac{p_{\perp}^2}{2m^2 c^2} F_0(p_x, p_{\perp}^2), \quad (51)$$

$$\frac{T_{\parallel}}{mc^2} = \int_0^{+\infty} dp_{\perp} 2\pi p_{\perp} \int_{-\infty}^{+\infty} dp_x \frac{p_x^2}{m^2 c^2} F_0(p_x, p_{\perp}^2). \quad (52)$$

Specifically, by introducing the distribution (49) used within our model, Eqs. (51) and (52) lead to

$$\frac{T_{\perp}}{mc^2} = \sum_{r=0}^{N_{ring}} \frac{\alpha_r \beta_{\perp r}^2 \Gamma_{ar} G(\beta_{ar})}{2} = \sum_{r=0}^{N_{ring}} \frac{\alpha_r T_{\perp r}}{mc^2}, \quad (53)$$

$$\frac{T_{\parallel}}{mc^2} = \sum_{r=0}^{N_{ring}} \alpha_r \Gamma_{ar} [1 - (1 - \beta_{ar}^2) G(\beta_{ar})] = \sum_{r=0}^{N_{ring}} \frac{\alpha_r T_{\parallel r}}{mc^2}, \quad (54)$$

where $T_{\perp r}$ and $T_{\parallel r}$ defined by Eqs. (53) and (54), respectively, define the perpendicular and parallel temperatures associated with the ring of label r . First notice that $T_{\parallel r} \rightarrow 0$ and $\frac{T_{\perp r}}{mc^2} \rightarrow \frac{C_{\perp r}^2}{2m^2 c^2 \Gamma_{ar}}$ when $\beta_{ar} \rightarrow 0$ (or equivalently when the function $G(\beta_{ar}) \rightarrow 1$).

For a single ring with $N_{ring} = 1$, Eq. (50) can be expressed in a dimensionless and polynomial form:

$$-\omega^4 + \omega^2(\omega_k^2 + k^2 \beta_{a1}^2 - A_{\perp}) - k^2 \beta_{a1}^2 \omega_k^2 + A_{\perp} k^2 = 0, \quad (55)$$

where $A_{\perp} = \frac{\alpha_1 C_{\perp}^2}{2\Gamma_{a1}(1+C_{\perp}^2)}$ and where we have replaced $\frac{C_{\perp}}{mc}$ by C_{\perp} to describe the ring's size. The corresponding instability condition for Eq. (55) yields now to

$$\beta_{a1}^2 \omega_k^2 < \frac{\alpha_1 C_{\perp}^2}{2\Gamma_{a1}(1+C_{\perp}^2)} = \frac{(1-\alpha_0)\beta_{\perp 1}^2}{\Gamma_{a1}(1-\beta_{a1}^2)}, \quad (56)$$

which depends explicitly of the effective density of the central stream.

We choose $C_{\perp} = p_{th,\perp} \simeq 3.426mc$ for a temperature of $T_{\perp} \sim 840\text{keV}$. As a numerical example, shown in Fig. 5, is the plot of the growth rate $\frac{\Gamma}{\omega_p}$ against $\frac{kx}{\omega_p}$ for different values of the effective density α_0 from 0.1 till 0.6. It is evident from Fig. 5 that the growth rate strongly decreases when the density of the central beam increases. Thus a stabilization process is observed when $\alpha_0 \geq 0.80$, showing that the shape

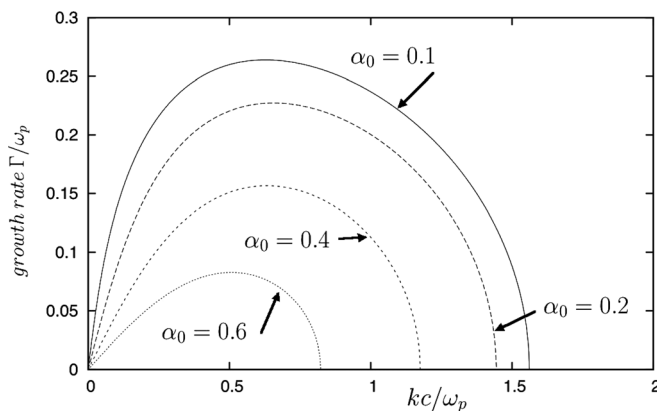


FIG. 5. Typical plot of the growth rate $\frac{\Gamma}{\omega_p}$ against $\frac{kx}{\omega_p}$ for a ring-type distribution in the perpendicular momentum space for WI. A stabilization process is observed when the effective density of the central beam α_0 is greater than 0.8 indicating that the global shape of the distribution plays a key role in WI.

of the distribution plays a central role in WI. Applications of these results are left to paper II where the study of the asymptotic stationary equilibrium will be studied in the case of circularly polarized wave.

VIII. CONCLUSION

This first part of a series of articles on the Hamiltonian multistream model describes the linear and relativistic regime of Weibel-type instabilities. Specifically, the multistream model, or its “multiring” extension for circularly polarized waves, is a set of one-dimensional reduced Vlasov-type equations obtained in a Hamiltonian framework when one spatial dimension is lacking allowing the use of the invariance property of the canonical momentum in a perpendicular direction. By approximating the system as a finite number of particle “bunches” or “streams,” or in other words, as a summation of Dirac distributions, we have obtained the linear dispersion relation of the Weibel instability in the relativistic regime when a temperature anisotropy is taken into account. Although a simplification is introduced in the analytical treatment by using a water-bag description in the parallel direction in momentum space, the model can be extended to a more general situation without difficulty. This formulation gives also a clear description of the temperature effects in the relativistic regime of the instability and there are no constraints on the shape of the equilibrium distribution which can be far from the relativistic Maxwell-Jüttner equilibrium.

For the case of a dissymmetric distribution, it has been shown that the dispersion relation possesses two branches, one of the purely electromagnetic character (i.e., transverse) and another of a purely electrostatic nature leading to a possible mixed electrostatic-electromagnetic nature. Our analytical model can be used without difficulty to study the linear coupling between filamentation and Weibel instabilities leading to a cumulative effect of both instabilities.

From the analytical and numerical treatment of the problems of interest of this paper, the multistream formalism is more appropriate. This is particularly true for the numerical simulations since the Vlasov-Maxwell formalism is cast into a four-dimensional phase space, while the multistream model only requires the discretization of a two-dimensional phase space plus the introduction of a limited number of streams. Numerical simulations based on the multistream model are left to papers II and III where specific problems are addressed pertaining now to the nonlinear aspects of the instability where trapped particle populations play a key role in the saturation process of the Weibel instability.

ACKNOWLEDGMENTS

The authors are indebted to the IDRIS computational center, Orsay, France, for computer time allocation on their computers.

APPENDIX A: POLYNOMIAL FORM OF THE DISPERSION RELATION IN THE WATER-BAG APPROACH

In the multistream approach, the equilibrium state is described by the set of parameters $\{\alpha_j, C_j, p_{aj}\}$ for $|j| \leq N$,

corresponding to a plasma description in terms of $2N+1$ streams, each stream keeping its initial perpendicular momentum C_j in the perpendicular direction p_y , constant in time. Furthermore we used here normalized quantities: momentum $p_{x/y}$ or C_j , wave vector k , and frequencies ω being normalized to mc , ω_p/c and ω_p respectively. Choosing for each stream $p_{aj} = p_a$, independent of j (but keeping in mind that $\beta_{aj} = p_a/\Gamma_{aj}$ depends explicitly of C_j by the Lorentz factor $\Gamma_{aj} = \sqrt{1 + p_a^2 + C_j^2}$), the set of parameters $\{\alpha_j, C_j\}$ is then determined through the resolution of the following system:

$$\sum_{j=1}^N 2\alpha_j C_j^{2n} \langle \gamma_{aj}^{-1} \rangle = \left\langle \frac{p_y^{2n}}{\gamma} \right\rangle \quad \text{for } n = 1, 2, \dots \quad (\text{A1})$$

We keep for the central stream the condition $C_0 = 0$ and the parameter α_0 must be calculated from the normalization condition $\sum_{j=-N}^{+N} \alpha_j = 1$. The right-hand side of Eq. (A1) is then determined numerically by the following relation:

$$\left\langle \frac{p_y^{2n}}{\gamma} \right\rangle = \frac{\int_{-\infty}^{+\infty} dp_y \frac{p_y^{2n} \exp(-\mu \sqrt{1 + p_y^2}) G(p_y)}{\sqrt{1 + p_y^2 + p_{aj}^2}}}{\int_{-\infty}^{+\infty} \exp(-\mu \sqrt{1 + p_y^2}) dp_y}. \quad (\text{A2})$$

Thus, for a given number of streams, the set of parameters $\{\alpha_j, C_j, p_{aj}\}$ is used for the resolution of the dispersion relation given in Eq. (29) which corresponds to the pure transverse Weibel instability.

The determination of quantities $\{\alpha_j, C_j, p_{aj}\}$ for $|j| \leq 3$ is made by solving Eqs. (A1) and the condition of normalization $\sum_{j=-3}^3 \alpha_j = 1$, using the analytical expression (A2) to calculate the moment of order $2n$ of the quantity $\langle p_y^{2n}/\gamma \rangle$ till $n=6$. The corresponding polynomial expression of the dispersion relation can be easily obtained and writes as

$$\begin{aligned} \omega^8 - \omega^6 \left(k^2 \sum_{j=1}^3 \beta_{aj}^2 + \omega_k^2 - 2 \sum_{j=1}^3 A_j \right) \\ + \omega^4 \left[k^4 \sum_{i<j} \beta_{ai}^2 \beta_{aj}^2 + \omega_k^2 k^2 \sum_{j=1}^3 \beta_{aj}^2 \right. \\ \left. - 2k^2 \sum_{j=1}^3 A_j \left(\sum_{i \neq j} \beta_{aj}^2 \right) - 2k^2 \sum_{j=1}^3 A_j \right] \\ + \omega^2 \left[2k^4 \sum_{j=1}^3 A_j \left(\prod_{i \neq j} \beta_{ai}^2 \right) + 2k^4 \sum_{j=1}^3 A_j \left(\sum_{i \neq j} \beta_{ai}^2 \right) - k^6 \prod_{j=1}^3 \beta_{aj}^2 \right. \\ \left. - k^4 \omega_k^2 \sum_{i<j} \beta_{ai}^2 \beta_{aj}^2 + k^6 \omega_k^2 \prod_{j=1}^3 \beta_{aj}^2 \right] - 2k^6 \sum_{j=1}^3 A_j \left(\prod_{i \neq j} \beta_{ai}^2 \right) = 0, \end{aligned} \quad (\text{A3})$$

where the coefficients A_j are determined by

$$A_j = \frac{\alpha_j C_j^2}{\Gamma_{aj} (1 + C_j^2)}. \quad (\text{A4})$$

APPENDIX B: DIELECTRIC TENSOR ELEMENTS $\epsilon_{\alpha\beta}$

Inserting the perturbation field term as $\delta \mathbf{A}_\perp = \delta A_y \mathbf{e}_y + \delta A_z \mathbf{e}_z$ into Eqs. (23) and (24) and taking the determinant of the obtained system equal to zero yields to the calculation of the tensor elements. They are expressed without any approximation in term of the set of parameters $\{\alpha_j, C_j, p_{aj}\}$

$$\epsilon_{xx} = 1 - \omega_p^2 \sum_{j=-N}^{+N} \frac{\alpha_j}{\Gamma_{aj} (\omega^2 - k^2 v_{aj}^2)}, \quad (\text{B1})$$

$$\epsilon_{x\beta} = \epsilon_{\beta x} = -ik \omega_p^2 \sum_{j=-N}^{+N} \frac{\alpha_j C_{\beta j}}{m \Gamma_{aj}^2 (\omega^2 - k^2 v_{aj}^2)} \quad \text{for } \beta = y, z, \quad (\text{B2})$$

$$\begin{aligned} \epsilon_{\beta\beta} = \omega_p^2 \sum_{j=-N}^{+N} \frac{\alpha_j C_{\beta j}^2}{m^2 c^2 \Gamma_{aj} \left(1 + \frac{C_{\perp j}^2}{m^2 c^2} \right)} - \omega^2 + k^2 c^2 \\ + \omega_p^2 \sum_{j=-N}^{+N} \alpha_j \langle \gamma_{aj}^{-1} \rangle \\ - k^2 \omega_p^2 \sum_{j=-N}^{+N} \frac{\alpha_j C_{\beta j}^2}{m^2 \Gamma_{aj}^3 (\omega^2 - k^2 v_{aj}^2)} \quad \text{for } \beta = y, z, \end{aligned} \quad (\text{B3})$$

$$\begin{aligned} \epsilon_{\alpha\beta; \alpha\beta \neq x \neq \beta} = -\omega_p^2 \sum_{j=-N}^{+N} \frac{\alpha_j C_{\alpha j} C_{\beta j}}{m^2 c^2 \Gamma_{aj} \left(1 + \frac{C_{\perp j}^2}{m^2 c^2} \right)} \\ + \omega_p^2 k^2 \sum_{j=-N}^{+N} \frac{\alpha_j C_{\alpha j} C_{\beta j}}{m^2 \Gamma_{aj}^3 (\omega^2 - k^2 v_{aj}^2)}. \end{aligned} \quad (\text{B4})$$

¹E. W. Weibel, *Phys. Rev. Lett.* **2**, 83 (1959).

²B. D. Fried, *Phys. Fluids* **2**, 337 (1959).

³M. V. Medvedev, *Astrophys. J.* **651**, L9 (2006).

⁴M. V. Medvedev and A. Loeb, *Astrophys. J.* **526**, 697 (1999).

⁵R. Schlickeiser and P. K. Shukla, *Astrophys. J.* **599**, L57 (2003).

⁶M. Lazar, R. Schlickeiser, R. Wielebinski, and S. Poedts, *Astrophys. J.* **693**, 1133 (2009).

⁷M. V. Medvedev, L. O. Silva, and M. Kamionkowski, *Astrophys. J.* **642**, L1 (2006).

⁸P. Yoon and R. C. Davidson, *Phys. Rev. A* **35**, 2718 (1987).

⁹D. C. DePackh, *J. Electron. Control* **13**, 417 (1962).

¹⁰P. Bertrand, J. P. Doremus, G. Baumann, and M. R. Feix, *Phys. Fluids* **15**, 1275 (1972).

¹¹P. Bertrand, M. Albrecht-Marc, T. Reveille, and A. Ghizzo, *Transp. Theory Stat. Phys.* **34**, 103 (2005).

¹²A. Inglebert, A. Ghizzo, T. Reveille, D. Del Sarto, P. Bertrand, and F. Califano, *Plasma Phys. Controlled Fusion* **54**, 085004 (2012).

¹³A. Inglebert, A. Ghizzo, T. Reveille, P. Bertrand, and F. Califano, *Phys. Plasmas* **19**, 122109 (2012).

¹⁴M. Lazar, M. E. Dieckmann, and S. Poedts, *J. Plasma Phys.* **76**, 49 (2010).

¹⁵M. Lazar, R. Schlickeiser, and P. K. Shukla, *Phys. Plasmas* **13**, 102107 (2006).

¹⁶A. Ghizzo, *Phys. Plasmas* **20**, 082110 (2013).

¹⁷I. Bernstein, J. Greene, and M. D. Kruskal, *Phys. Rev.* **108**, 546 (1957).

¹⁸A. Ghizzo, *Phys. Plasmas* **20**, 082111 (2013).

¹⁹A. Ghizzo, P. Bertrand, M. M. Shoucri, T. W. Johnston, E. Fijalkow, and M. R. Feix, *J. Comput. Phys.* **90**, 431 (1990).

²⁰P. Bertrand, A. Ghizzo, T. W. Johnston, M. Shoucri, E. Fijalkow, and M. R. Feix, *Phys. Fluids B* **2**, 1028 (1990).

- ²¹F. Huot, A. Ghizzo, P. Bertrand, E. Sonnendrücker, and O. Coulaud, [IEEE Trans. Plasma Sci.](#) **28**, 1209 (2000).
- ²²M. R. Feix and P. Bertrand, [Transp. Theory Stat. Phys.](#) **34**, 7 (2005).
- ²³F. Pegoraro, S. V. Bulanov, F. Califano, and M. Lontano [Phys. Scr.](#) **T63**, 262 (1996).
- ²⁴R. Schlickeiser, [Phys. Plasmas](#) **11**, 5532 (2004).
- ²⁵A. Bret, L. Gremillet, and J. C. Bellido, [Phys. Plasmas](#) **14**, 032103 (2007).
- ²⁶M. Tzoufras, C. Ren, F. S. Tsung, J. W. Tonge, W. B. Mori, M. Fiore, R. A. Fonseca, and L. O. Silva, [Phys. Rev. Lett.](#) **96**, 105002 (2006).